Pseudo-Two-Dimensional Structures $(HXYH)_{3n^2}H_{6n}$ (XY = GaN, SiC, GeC, SiSi, or GeGe; $n = 1-3$): Density Functional Characterization of Structures and Energetics†

Bethany L. Kormos, Christopher J. Cramer,* and Wayne L. Gladfelter*

Department of Chemistry and Supercomputing Institute, University of Minnesota, 207 Pleasant Street SE, Minneapolis, Minnesota 55455

Received: April 11, 2005; In Final Form: June 17, 2005

Hybrid density functional calculations with effective core potential basis sets are performed for monomeric group 13/15 and group 14/14 analogues of cyclohexane, as well as for three different pseudo-two-dimensional structures that can be formed from expanding one and two concentric rings around the central one (trans-fused chairs, a rolling combination of trans- and cis-fused chairs, and cis-fused boats). Varying contributions from torsional strain, angle strain, electrostatics, and nontraditional H−H hydrogen bonding lead to different orderings and magnitudes of motif energies in the various systems: Homoatomic SiSi and GeGe systems prefer the trans-fused chair alternative and heteroatomic systems GaN, SiC, and GeC prefer the rolling chair. Decomposition of structure energies into characteristic fragment contributions indicates that pseudo-one-dimensional rods of poly(imidogallane) are thermodynamically more stable than any of the pseudo-two-dimensional structures.

1. Introduction

Group 13−15 semiconductor materials such as GaN may be employed in the construction of such optoelectronic devices as light emitting diodes and blue lasers.[1,2] Considerable additional interest has been provoked by recent syntheses of various GaN structures on the nanoscale.[3]

Prior work[4,5] described a method for controlling the particle size and phase of GaN materials and reported the isolation of imidogallane, $[HGaNH]_n$, **1**, as a stable intermediate in the ammonothermal conversion of $[H_2GaNH_2]_3$ to GaN. The structure originally proposed for $[HGaNH]_n$ was that of a puckered sheet of six-membered rings all in chair conformations and connected by trans-diequatorial Ga−N bonds at all ring junctions.

We recently reevaluated that suggestion based on experimental structural characterization of various relevant clusters, such as $[(PhGa)_7(NMe)_5(NHMe)_4)]$,[6,7] and on computational studies of analogous rodlike oligomers of $[HGaNH]_n$.[8] Such oligomers were theoretically predicted to have distinct optical excitation energies, the energy separation between which was found to be in good accord with band separations observed in experimental fluorescence spectra of $[HGaNH]_n$. We interpreted these data to imply that imidogallane prepared as described above consists not of puckered sheets but rather of a collection of oligomeric rods of six-membered HGaNH rings that are stacked axially as chairs one atop the next (i.e., having a pseudo-one-dimensional wurtzite structure).

A question of some interest, however, is whether pseudo-*two*-dimensional structures, like that originally proposed for $[HGaNH]_n$, could indeed be accessed under different sets of experimental conditions. This paper considers three possible such structures: the one originally proposed for $[HGaNH]_n$, an alternative in which adjacent chains of trans-diequatorially fused chairs are connected by cis-axial/equatorial ring junctions, and another alternative in which the six-membered rings are fused to one another as boats (Figure 1; we will refer to these three alternatives as the flat-chair (FC), rolling-chair (RC), and flat-boat (FB) structural motifs). We employ density functional theory to examine the structures and energetics of these systems and we make comparisons to rodlike $[HGaNH]_n$ oligomers as well as to analogous group 14−14 structures incorporating second- and third-row atoms in order to gain insight into the origin of structural preferences in these systems.

2. Computational Methods

All molecular structures $(HXYH)_{3n^2}H_{6n}$ (XY = GaN, SiC, GeC, SiSi, GeGe; $n = 1-3$) were fully optimized using the B3LYP[9] hybrid density functional which combines[10] the generalized gradient approximation (GGA) exchange functional of Becke[11] with exact Hartree−Fock exchange[12] and the Lee, Yang, and Parr GGA correlation functional.[13] This functional has previously been demonstrated to give excellent results for the prediction of structural and energetic quantities in monomeric and oligomeric group 13/15 and group 14/14 compounds including gallazane monomers and dimers.[8,14,15]

For geometry optimizations, B3LYP was used in conjunction with one or more of three different basis set combinations depending on the size of the system. We denote the largest basis set as CEP* and it is defined as the CEP-31G basis[16−18] with a 28-electron effective core potential (ECP) on Ge augmented with a single set of d functions having exponent 0.2, the CEP-31G basis with a 10-electron ECP on Ga (the looser split valence 3d functions that are included with the 10-electron ECP can serve as polarization functions for this atom, in contrast to the case for Ge), the CEP-31G(d) basis with a 10-electron ECP on Si, the CEP-31G(d) basis with 2-electron ECPs on N and C, and the 3-21G basis[19] on H. A somewhat smaller basis, which we denote as CEP, removes the polarization functions from Ge, Si, N, and C but is otherwise equivalent to CEP*—results for this basis are for the most part not reported in the interests of brevity. Our smallest basis set/ECP combination, hereafter called

† Part of the special issue "Donald G. Truhlar Festschrift".

10.1021/jp051885+ CCC: $33.50
Published on Web 07/28/2005

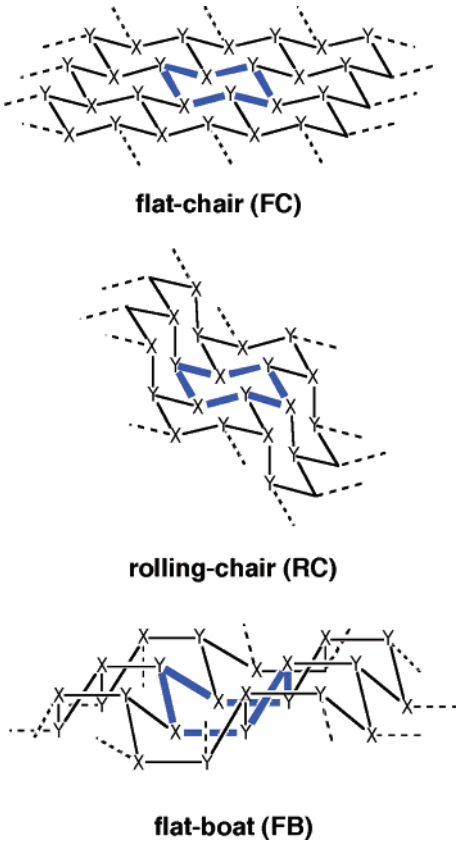

Figure 1. The flat-chair (FC), rolling-chair (RC), and flat-boat (FB) structures generated by different ring annelation schemes to a central chair conformer in the first two cases and a central boat conformer in the third case (central conformers are in blue). X and Y refer to the relevant heavy atoms. Heavy-atom−heavy-atom bonds that would extend the illustrated structures in larger systems are indicated by dashed lines. Hydrogen atoms cap all fourth valences but are not illustrated for clarity.

MB, employs the Hay-Wadt[20−22] minimal basis set with 28-electron ECPs for Ga and Ge and a 10-electron ECP for Si, and the STO-3G basis set[23,24] for N, C, and H. All $n = 1$ and $n = 2$ optimized geometries were confirmed as minima by computation of analytic second derivatives.

Single-point B3LYP/CEP* energy calculations were performed on structures optimized with the smaller basis sets (e.g., B3LYP/CEP*//B3LYP/MB) to assess the energetic consequences of using these geometries for the largest structures. Comparisons were made to structural and energetic data computed at the MP2/pVDZ[14b] or B3LYP/CEP* levels. All electronic structure calculations were performed using Gaussian 98, Revision A.11.[25]

3. Results and Discussion

3.1. Structures of Parent Six-Membered Rings. Three different conformers of the $n = 1$ systems {$[HXYH]_3H_6$, XY = GaN, SiC, GeC, SiSi, GeGe}, chair, boat, and twist-boat (Figure 2), were computed at the B3LYP/CEP*, B3LYP/CEP, and B3LYP/MB levels of theory and compared to available experimental structures. Heavy-atom bond lengths, angles and dihedrals for these optimized structures at the B3LYP/CEP* level can be found in Table 1. For the compounds in which XY = GaN, SiC and GeC, the computed chair, boat, and twist-boat structures have C_{3v}, C_s and C_1 symmetry, respectively; for the X = Y = Si and Ge compounds, the computed chair, boat, and twist-boat structures have D_{3d}, C_{2v} and C_2 symmetry,

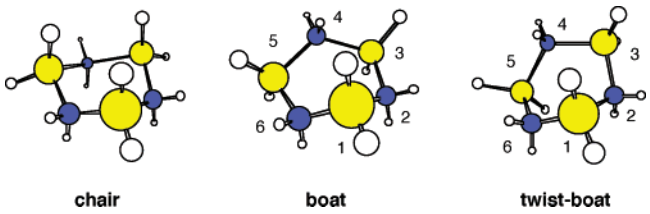

Figure 2. Chair, boat, and twist-boat conformations for [H2GaNH2]3 six-membered rings. Atom-numbering is provided where needed for Tables 1, 2, and 3. In Tables 2 and 3, chair atoms X1 and Y4 are those that are axially substituted by Y and X atoms, respectively, in RC extended sheets, while the other four ring atoms are equatorially substituted (see Figure 1 for RC sheet structure).

respectively. Only unique bond lengths, angles, and dihedrals are tabulated. Experimental structures available for comparison are the chair conformations of $[H_2GaNH_2]_3$ (single-crystal X-ray diffraction),[14b] $[H_2SiCH_2]_3$ (gas-phase electron diffraction),[26] and $[H_2GeCH_2]_3$ (single-crystal X-ray diffraction)[27] and all three conformations for $[H_2SiSiH_2]_3$ (gas-phase electron diffraction).[28] In the crystal structures, deviations from ideal symmetry were sometimes observed. To simplify comparison of the experimental and computed data, Table 1 lists average experimental values for such parameters.

Comparisons between the theoretical predictions and the available experimental data are for the most part quite good. Theory systematically overestimates the heavy atom bond lengths by 0.03 to 0.05 Å. However, as discussed further below, the energetic consequence of this overestimation appears to be quite small when comparisons of relative isomeric energies are made.

Comparisons between the various structures are also of some interest. For the various chair species, experimental bond lengths increase as Si−C < Ge−C < Ga−N < Si−Si (while not yet measured, it is likely that the Ge−Ge bond lengths will be longer than the Si−Si bond lengths, given that Ge−C bond lengths are longer than Si−C analogues, and that third-row germanium has a larger covalent radius than second-row silicon). This ordering is entirely consistent with tabulated covalent atomic radii for C, N, Si, Ga, and Ge of 0.77, 0.75, 1.11, 1.26, and 1.22 Å, respectively.[29] The computed bond lengths follow the same trend within *every* conformation.

With respect to valence bond angles, theory and experiment agree that when X and Y are different atoms and have different electronegativities, the X−Y−X angles are consistently larger than the Y−X−Y angles. This observation is in keeping with Bent's Rule,[30] which states that an atom devotes less s character and more p character to its bonding hybrid orbitals, thereby decreasing valence bond angles, as the electronegativity of the substituents increases. For example, nitrogen is more electronegative than hydrogen which is more electronegative than gallium (N = 3.04, H = 2.20, Ga = 1.81, Pauling electronegativity scale[31]), so Ga devotes more s character to its bonds to H and more p character to its bonds to N resulting in a rather small N−Ga−N angle of, for instance, 99.8 deg in the chair conformer. By contrast, N devotes more s character to Ga and more p to H and this leads to a significantly larger Ga−N−Ga angle, e.g., 119.4 deg in the chair conformer. The same trend is present in the boat and twist-boat conformers as well. This electronegativity-based variation in valence bond angles is also seen in the SiC and GeC systems, although the differences in these compounds are smaller because the differences in electronegativity are considerably smaller (C = 2.55, Si = 1.90, Ge = 2.01[31]).

TABLE 1: B3LYP/CEP* and Experimental[a] Bond Lengths *r*, (Å), Valence Bond Angles ∠, (deg), and Dihedral Angles *ω*, (deg) for $[HXYH]_3H_6$ Rings, XY = GaN, SiC, GeC, SiSi, or GeGe[b]

structural parameter	X = Ga, Y = N	X = Si, Y = C	X = Ge, Y = C	X,Y = Si	X,Y = Ge
			Chair		
*r*XY	2.030 (1.978)	1.906 (1.872)	1.975 (1.951)	2.375 (2.342)	2.468
∠XYX	119.4 (117.1)	113.8 (113.0)	113.6 (112.2)	110.3 (110.3)	110.5
∠YXY	99.8 (100.3)	110.2 (110.7)	110.1 (109.8)		
*ω*XYXY	60.5	53.3	53.6	58.0 (57.8)	57.4
			Boat		
*r*X1Y2	2.024	1.904	1.973	2.375 (2.342)	2.468
*r*Y2X3	2.032	1.917	1.984	2.389 (2.342)	2.478
*r*X3Y4	2.023	1.908	1.976		
*r*HH (flagpole)	2.630	2.962	3.046	3.373	3.423
∠X1Y2X3	119.0	114.1	114.0	111.7 (113.8)	111.7
∠X3Y4X5	119.9	114.5	114.1	110.3 (113.8)	110.8
∠Y2X3Y4	101.4	111.5	111.3		
∠Y2X1Y6	99.9	110.2	110.2		
*ω*X1Y2X3Y4	9.6	3.2	2.6	0.0 (0.0)	0.0
*ω*Y2X3Y4X5	−56.6	−48.9	−50.0	−55.2 (−47.7)	−54.9
*ω*Y6X1Y2X3	61.1	53.1	53.1		
			Twist Boat		
*r*X5Y6	2.026	1.912	1.980	2.381 (2.342)	2.472
*r*Y6X1	2.024	1.905	1.974	2.374 (2.342)	2.467
*r*X1Y2	2.030	1.911	1.979	2.382 (2.342)	2.474
*r*HH (flagpole)	2.960	3.290	3.402	3.827	4.004
∠X1Y2X3	118.9	114.1	114.0	111.9 (108.4)	111.6
∠X1Y6X5	117.0	113.1	113.1	110.2 (108.4)	110.6
∠Y2X1Y6	100.3	110.6	110.5	110.2 (108.4)	110.6
∠Y4X5Y6	99.4	111.3	111.1	111.8 (108.4)	111.6
*ω*Y6X1Y2X3	30.0	29.1	29.2	31.7 (34.3)	31.4
*ω*Y2X3Y4X5	−73.1	−61.5	−61.9	−66.1 (−73.7)	−65.7
*ω*X3Y4X5Y6	38.7	30.2	30.3	31.7 (34.3)	31.4

[a] References 14b (GaN), 26 (SiC), 27 (GeC), and 28 (SiSi). [b] Experimental data in parentheses after predicted data.

The large disparity in X−Y−X vs Y−X−Y valence bond angles in the GaN system causes substantial puckering of the six-membered ring compared to the other structures. Thus, the ring dihedral angles in the GaN ring are systematically larger than in the other rings for all conformers.

A final trend that is worthy of note is the flagpole H−H distance in the GaN boat and twist-boat conformers compared to the isoelectronic SiC system. Even though the GaN bond lengths are roughly 0.1 Å longer than the SiC bond lengths, the flagpole H separation is about 0.33 Å smaller in the GaN conformers than in the SiC analogues. Part of this shortening may be attributed to the unconventional H−H hydrogen bonding interaction that is present in the GaN rings, where one flagpole hydrogen has hydride character and the other has proton character.[14,32] This interaction, which is predominantly electrostatic in nature,[33] is sufficiently strong that the twist-boat conformer is lower in energy than the chair conformer for the GaN system,[14b] in contrast to every other XY combination studied here (vide infra).

3.2. Structural Effects of One Increment of Pseudo-Two-Dimensional Expansion. To form the $n = 2$ systems, $[HXYH]_{12}H_{12}$, a single set of six rings is attached concentrically around the $n = 1$ systems. Addition of these rings to the chair conformation can be accomplished two different ways, creating either a trans-fused (FC) or cis-fused (RC) network; addition to the boat conformation can be accomplished in only one manner (FB). Structural data for the central rings of the $n = 2$ systems computed at B3LYP/CEP* level can be found in Table 2. The FC, RC, and FB structures have C_{3v}, C_s, and C_s symmetry, respectively, for the GaN, SiC, and GeC compounds, and D_{3h}, C_{2h}, and C_{2v} symmetry, respectively, for the SiSi and GeGe compounds. Only unique bond lengths, angles and dihedrals are tabulated.

TABLE 2: B3LYP/CEP* Bond Lengths *r*, (Å), Valence Bond Angles ∠, (deg), and Dihedral Angles *ω*, (deg) for the Central Ring of $[HXYH]_{12}H_{12}$ Sheets, XY = GaN, SiC, GeC, SiSi, or GeGe

structural parameter	X = Ga, Y = N	X = Si, Y = C	X = Ge, Y = C	X,Y = Si	X,Y = Ge
			FC		
*r*XY	2.014	1.915	1.989	2.385	2.487
∠XYX	114.0	112.4	112.4	111.1	111.4
∠YXY	105.8	111.1	110.8	111.1	111.4
*ω*XYXY	59.0	53.9	54.3	55.8	54.8
			RC		
*r*X1Y2	2.018	1.917	1.991	2.386	2.489
*r*Y2X3	1.974	1.906	1.980	2.382	2.481
*r*X3Y4	2.008	1.913	1.987		
∠X1Y2X3	114.4	113.4	113.1	110.8	111.1
∠X3Y4X5	108.7	111.5	111.3	111.1	111.4
∠Y2X3Y4	103.5	110.7	110.5		
∠Y2X1Y6	105.8	111.4	111.2		
*ω*X1Y2X3Y4	62.5	53.8	54.3	56.2	55.5
*ω*Y2X3Y4X5	69.3	56.4	57.0	56.4	55.6
*ω*Y6X1Y2X3	54.6	50.6	51.2		
			FB		
*r*X1Y2	1.985	1.911	1.984	2.382	2.485
*r*Y2X3	2.002	1.926	1.999	2.400	2.501
*r*X3Y4	2.001	1.912	1.986		
*r*HH (flagpole)	2.783	2.701	2.792	3.276	3.404
∠X1Y2X3	116.1	113.2	113.1	111.9	111.9
∠X3Y4X5	108.8	111.1	111.0	111.0	111.5
∠Y2X3Y4	105.0	111.6	111.1		
∠Y2X1Y6	108.7	111.7	111.7		
*ω*X1Y2X3Y4	6.9	2.0	2.4	0.0	0.0
*ω*Y2X3Y4X5	−67.4	−55.0	−56.2	−54.2	−53.9
*ω*Y6X1Y2X3	47.9	50.4	50.6		

Comparing the $n = 1$ to $n = 2$ systems, several key trends are evident. First, in all systems other than GaN, the heavy-

atom bond lengths in the central ring become 0.01 to 0.02 Å longer with cycloannelation. In the GaN system, by contrast, the bond lengths shorten by from 0.01 to 0.03 Å depending on conformer.

While it is tempting to assign this unique behavior to increasing ionic character in the GaN sheet as it grows, such speculation may not be justified. Instead, the bond length changes may be associated with valence bond angle changes that appear to be forced on the system by cycloannelation. The very large differences in the Ga−N−Ga and N−Ga−N bond angles present in the individual $n = 1$ ring conformers are substantially reduced in every $n = 2$ conformer. Reduced angles at Ga require additional s character in that atom's bonding hybrids to N, which would be expected to shorten the Ga−N bonds. Of course, the converse is true for N, so it is difficult to predict the final effect. In any case, it is clear that cycloannelation introduces significant strain in the GaN sheets compared to the others based on the changes induced in the central ring geometry.

Another indicator of the magnitude of the central ring distortion is the change in flagpole H−H distance in the $n = 2$ FB structure compared to the $n = 1$ boat structure. In all systems other than GaN the distance *decreases* by about 0.6 Å, as the constraints of cycloannelation offset any increased steric interaction. In the GaN system, on the other hand, the distance *increases* by 0.153 Å, as the constraints of cycloannelation force a decrease in the degree to which this favorable interaction can be enjoyed.

Indeed, as discussed in more detail below, the intrinsic preference of the GaN system to maintain large bond angle variations and ring puckering lead to substantial distortion of the FC ring system away from a "flat" sheet, as is found for all of the other systems, and instead curvature begins to develop.

3.3. Structural Effects of Two Increments of Pseudo-Two-Dimensional Expansion. Formation of the $n = 3$ systems, $[HXYH]_{27}H_{18}$, is accomplished by addition of a third concentric torus of six-membered rings to the three $n = 2$ systems in a continuation of the FC, RC, and FB motifs. For these largest systems, structural optimization at the B3LYP/CEP* level was impractical, and instead optimizations were carried out at the B3LYP/MB level of theory. As our interest is in qualitative geometric trends as a function of sheet size, and as B3LYP/MB calculations in general well reproduce the trends predicted at the B3LYP/CEP* level for $n = 1$ and $n = 2$ (data not shown), we consider this approach to be acceptable. Table 3 thus compares structural data for the central ring of the $n = 1-3$ systems computed at the B3LYP/MB level for all systems. The data for the central rings of the $n = 3$ structures should be most representative of what would be observed for an infinite two-dimensional sheet since edge effects are minimized. As in the $n = 2$ structures, the FC, RC, and FB sheets have C_{3v}, C_s, and C_s symmetry, respectively, for the GaN, SiC, and GeC compounds, and D_{3h}, C_{2h}, and C_{2v} symmetry, respectively, for the SiSi and GeGe compounds. Only unique bond lengths, angles, and dihedrals are tabulated. Figure 3 provides the computed structures for the $n = 3$ SiC sheets, which are qualitatively representative of the shapes of all of the systems with the exception of GaN, which is discussed in more detail below.

Excluding GaN, the geometries of the various central rings in all systems, irrespective of connection motif, exhibit considerably smaller changes on going from $n = 2$ to $n = 3$ compared to going from $n = 1$ to $n = 2$. Indeed, many geometric parameters appear to be essentially converged. Thus, a reasonable estimate of *accurate* geometric data may likely be obtained from consideration of the $n = 2$ larger basis set data in Table 2, corrected for changes associated with going from $n = 2$ to $n = 3$ as listed in Table 3. We may assess this point for two known compounds, namely $[SiH]_n$ and $[GeH]_n$. Both have been determined from X-ray diffraction to consist of layers of FC sheets with lattice constants a (corresponding to the distance between heavy atoms 1,3-related to one another in a given ring) of 3.83[34] and 3.98[35] Å, respectively. The lattice constant a may be computed from the heavy atom bond lengths and the valence bond angle by the law of cosines. In the case of $[SiH]_n$, we take the SiSi bond length to be 2.386 Å (2.385 Å from Table 2 plus 0.001 Å for the change predicted on going from $n = 2$ to $n = 3$ in Table 3) and the valence bond angle to be 111.2 (by the analogous procedure); this predicts a to be 3.94 Å, in quite reasonable agreement with the bulk experimental value. The same procedure for $[GeH]_n$ leads to a predicted lattice constant a of 4.11 Å, which is again in good agreement with the experimental value (note that the difference between the Si and Ge systems is predicted almost quantitatively).

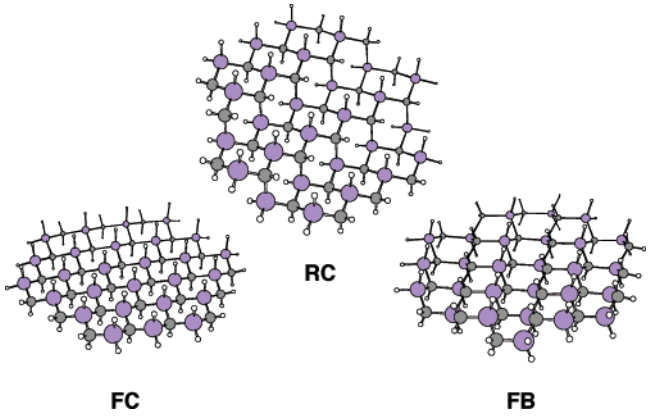

Figure 3. FC, RC, and FB structures for $[HSiCH]_{27}H_{18}$ optimized at the B3LYP/MB level.

With respect to particular trends observed in specific systems, all 3 Si−C and Ge−C motifs show for the most part slightly increased bond lengths and decreased valence bond angles in the largest sheet compared to the monomer. In addition, the H···H flagpole distances decrease in the RC and FB structures. There is, then, an overall puckering of the central ring as consecutive rings are added from $n = 1$ to $n = 3$. By contrast, the clusters in which X = Y = Si or Ge exhibit somewhat different trends. Most notably, all valence bond angles increase slightly, the dihedral angles decrease, and the H···H flagpole distances increase. Thus, the constituent rings in these systems become *less* puckered with increasing sheet size.

With respect to the GaN systems, there is a general tendency of the central ring in all structures to pucker more in the largest sheet than in the monomer, just as observed for the other heteroatomic ring systems. In the case of the FC structure, however, the MB basis set appears to do rather poorly with respect to the geometries of the outermost rings, i.e., edge effects depend significantly on basis set size.

This sensitivity in the FC system appears to be associated primarily with electrostatics. In the heteroatomic systems, one may consider each X−H and Y−H bond to carry a characteristic dipole moment. When the electronegativity of H lies between that of X and Y, as is the case in GaN, for example (vide supra), then the geometry of the FC system is such that all X−H bonds and Y−H bonds orthogonal to the sheet plane are parallel and moreover have their dipole moments all oriented in the same direction. Thus, in the monomer there are six such aligned

TABLE 3: B3LYP/MB Bond Lengths *r*, (Å), Valence Bond Angles ∠, (deg), and Dihedral Angles *ω*, (deg) for the Central Rings of $(HXYH)_{3n^2}H_{6n}$ Sheets, XY = GaN, SiC, GeC, SiSi, GeGe, *n* = 1-3

	GaN			SiC			GeC		
structural parameter	$n=1$	$n=2$	$n=3$	$n=1$	$n=2$	$n=3$	$n=1$	$n=2$	$n=3$
				FC					
*r*XY	1.994	1.983	1.989	1.967	1.974	1.975	2.035	2.049	2.050
∠XYX	124.6	118.9	113.2	112.5	111.5	111.3	113.4	112.0	111.8
∠YXY	106.6	111.6	108.1	111.8	110.9	110.7	111.7	110.8	110.5
*ω*XYXY	40.9	42.0	57.1	52.8	55.6	56.1	51.5	55.0	55.7
				RC					
*r*X1Y2	1.994	2.004	1.990	1.967	1.975	1.972	2.035	2.050	2.048
*r*Y2X3	1.994	1.959	1.949	1.967	1.958	1.958	2.035	2.029	2.028
*r*X3Y4	1.994	1.997	1.990	1.967	1.973	1.973	2.035	2.047	2.048
∠X1Y2X3	124.6	115.4	116.2	112.5	112.3	112.6	113.4	112.7	113.0
∠X3Y4X5	124.6	110.0	110.2	112.5	111.0	111.2	113.4	111.1	111.5
∠Y2X3Y4	106.6	104.1	106.0	111.8	110.5	110.9	111.7	110.1	110.7
∠Y2X1Y6	106.6	108.1	109.2	111.8	111.0	111.3	111.7	111.2	111.5
*ω*X1Y2X3Y4	40.9	58.9	56.3	52.8	55.4	54.5	51.5	55.1	54.0
*ω*Y2X3Y4X5	40.9	68.2	65.1	52.8	57.2	56.0	51.5	57.9	56.4
*ω*Y6X1Y2X3	40.9	49.9	46.9	52.8	53.1	52.4	51.5	52.1	51.5
				FB					
*r*X1Y2	1.995	1.978	1.972	1.965	1.968	1.967	2.034	2.041	2.041
*r*Y2X3	1.996	1.997	1.986	1.975	1.984	1.983	2.041	2.057	2.057
*r*X3Y4	1.992	1.989	1.979	1.965	1.969	1.969	2.033	2.043	2.042
*r*HH (flagpole)	3.373	2.861	2.816	3.140	2.770	2.775	3.348	2.910	2.933
∠X1Y2X3	122.8	116.9	115.0	113.2	113.0	112.9	114.0	113.4	113.3
∠X3Y4X5	123.0	110.2	111.5	112.7	110.8	110.9	113.7	111.0	111.2
∠Y2X3Y4	104.7	105.1	107.0	112.9	111.0	111.3	112.9	110.6	111.1
∠Y2X1Y6	104.5	110.7	111.1	112.0	111.4	111.0	112.0	111.8	111.2
*ω*X1Y2X3Y4	6.6	8.8	5.3	0.6	2.2	1.2	1.0	3.1	1.7
*ω*Y2X3Y4X5	−47.8	−67.0	−62.9	−50.1	−56.5	−55.5	−48.6	−57.3	−55.7
*ω*Y6X1Y2X3	48.5	43.3	47.9	51.0	51.2	52.3	49.7	49.9	51.1

	Si			Ge		
structural parameter	$n=1$	$n=2$	$n=3$	$n=1$	$n=2$	$n=3$
			FC			
*r*XX	2.494	2.484	2.485	2.633	2.636	2.640
∠XXX	106.2	109.1	109.2	106.4	109.6	109.2
*ω*XXXX	67.3	61.0	60.4	66.8	59.6	58.9
			RC			
*r*X1X2	2.494	2.479	2.479	2.633	2.633	2.633
*r*X2X3	2.494	2.462	2.465	2.633	2.608	2.614
∠X1X2X3	106.2	107.9	108.0	106.4	108.2	108.4
∠X3X4X5	106.2	109.5	109.8	106.4	110.5	110.6
*ω*X1X2X3X4	67.3	61.8	61.3	66.8	61.8	61.3
*ω*X2X3X4X5	67.3	62.8	62.4	66.8	60.3	59.9
			FB			
*r*X1X2	2.492	2.488	2.477	2.629	2.625	2.630
*r*X2X3	2.501	2.474	2.492	2.641	2.639	2.644
*r*HH (flagpole)	2.764	3.118	3.003	2.875	3.377	3.290
∠X1X2X3	107.7	109.5	109.0	107.3	110.1	109.9
∠X3X4X5	105.3	109.1	109.2	106.0	109.8	109.5
*ω*X1X2X3X4	0.0	0.0	0.0	0.0	0.0	0.0
*ω*X2X3X4X5	−65.3	−60.2	−61.0	−65.7	−59.0	−59.6

dipoles, in the $n = 2$ sheet there are 24, and in the $n = 3$ sheet there are 54 (the general formula is $6n^2$). Table 4 lists the sheet dipole moments for *all* systems to illustrate the importance of this phenomenon. For the $n = 1$ and 2 cases, B3LYP/CEP* dipole moments have been computed for both the B3LYP/CEP* and B3LYP/MB optimized geometries. For the $n = 3$ case, only B3LYP/MB geometries are available.

In nearly every case where geometries are available from both the smaller and larger basis sets, the computed dipole moments for the two structures are in good agreement, reflecting only slight geometric differences. This is *not* the case for the GaN FC system, however. Noting the discussion above of the number of X−H and Y−H dipole moments as a function of ring size, we might naively expect that the dipole moments of the $n = 2$ systems would be about four times larger than those for the monomer, and that the dipole moments of the $n = 3$ sheets would be somewhat more than double those for the $n = 2$ sheets. This prediction proves surprisingly accurate in the SiC and GeC systems, and also for the B3LYP/CEP* geometries on going from $n = 1$ (3.5 D) to $n = 2$ (11.4 D). This suggests that a dipole moment of about 25 D might be expected for the $n = 3$ FC sheet (i.e., a bit more than double the $n = 2$ dipole moment of 11.4 D). However, the trend predicted with the B3LYP/MB geometries is 2.7, 2.2, and 4.3 D, respectively, for $n = 1$, 2, and 3. At this level of theory, the geometries of the outermost rings distort significantly in a manner that reduces the overall dipole moment. As a smaller basis set is less suited to ionic character in the electronic structure, it is possible that this distortion is an artifact. To assess this, for the GaN FC $n = 3$ structure, we reoptimized the geometry at the B3LYP/CEP level

TABLE 4: B3LYP/CEP* Dipole Moments (D) of $(HXYH)_{3n^2}H_{6n}$ Sheets, XY = GaN, SiC, GeC, SiSi, or GeGe and $n = 1-3$[a]

	GaN			SiC			GeC		
	$n=1$	$n=2$	$n=3$	$n=1$	$n=2$	$n=3$	$n=1$	$n=2$	$n=3$
FC	3.5	11.4	15.5[b]	1.1	5.0		1.1	4.7	
	(2.7)	(2.2)	(4.3)	(1.0)	(4.7)	(10.0)	(1.0)	(4.5)	(10.0)
RC	3.5	8.5		1.1	3.2		1.1	3.0	
	(2.7)	(8.7)	(21.1)	(1.0)	(2.7)	(6.6)	(1.0)	(2.8)	(6.9)
FB	1.3	4.8		0.3	1.3		0.3	1.3	
	(1.0)	(4.4)	(10.0)	(0.3)	(1.1)	(2.4)	(0.3)	(1.1)	(2.5)

	Si			Ge		
	$n=1$	$n=2$	$n=3$	$n=1$	$n=2$	$n=3$
FB[c]	0.0	0.3		0.0	0.3	
	(0.1)	(0.3)	(0.1)	(0.0)	(0.3)	(0.2)

[a] Data reported for B3LYP/CEP* geometries above, and B3LYP/MB geometries in parentheses below unless otherwise indicated. [b] B3LYP/CEP geometry. [c] FC and RC dipole moments are all zero by symmetry.

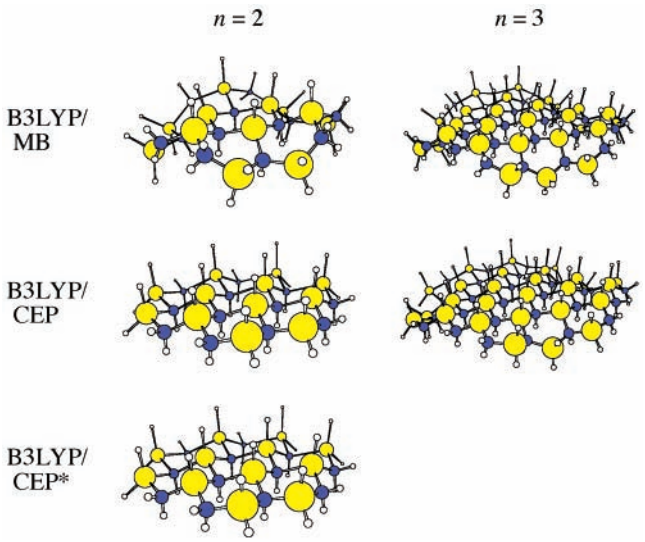

Figure 4. GaN FC $n = 2$ and $n = 3$ structures optimized at various levels.

TABLE 5: Curvature (Å^{-1}) and Radii of Curvature (Å) for $(HXYH)_{27}H_{18}$ FC Sheets, XY = GaN, SiC, or GeC[a]

XY	curvature κ	radius of curvature
GaN	0.107	9.385
	0.078[b]	12.771[b]
SiC	0.011	93.897
GeC	0.016	62.434

[a] For B3LYP/MB optimized structures unless otherwise indicated. [b] B3LYP/CEP optimized structure.

(Figure 4). The latter level gave good agreement with B3LYP/CEP* for the $n = 2$ congener, for which B3LYP/MB was already significantly distorted (Figure 4).

The degree to which the $n = 3$ FC structures distort in order to reduce the dipolar character of the electronic structure may be assessed from their curvature κ (which is simply the inverse of the radius of curvature, which may be computed from any 3 points in the structure; in this case we used an X atom of the central ring and the corresponding X atoms in rings at opposite ends in the outermost torus.) The FC curvatures are listed in Table 5 for the heteroatomic rings (the homoatomic rings have zero curvature by symmetry, which also guarantees that all heavy-atom-H dipole moments cancel). The curvatures become increasingly large with a greater electronegativity difference between X and Y. While the curvature of 0.107 Å^{-1} for GaN at the B3LYP/MB level is almost certainly overestimated, the B3LYP/CEP level still predicts a substantial value of 0.078 Å^{-1} (corresponding to a radius of curvature of 12.8 Å). It is interesting to speculate on whether suitably large structures could be induced to form nanoshells by taking advantage of this tendency to bend the FC sheet; the resulting shell would have an outer surface capped by hydride-like H atoms and an inner one capped by proton-like H atoms. However, we do not pursue this topic further here.

TABLE 6: Relative Energies (kcal mol^{-1}) of $(HXYH)_{3n^2}H_{6n}$ Sheets, XY = GaN, SiC, GeC, SiSi, or GeGe and $n = 1-3$[a]

	GaN			SiC			GeC		
	$n=1$	$n=2$	$n=3$	$n=1$	$n=2$	$n=3$	$n=1$	$n=2$	$n=3$
FC	2.7	14.7		0.0	0.3		0.0	0.1	
	(2.0)	(16.6)	(38.7)	(0.0)	(1.1)	(5.1)	(0.0)	(1.1)	(3.5)
RC	2.7	0.0		0.0	0.0		0.0	0.0	
	(2.0)	(0.0)	(0.0)	(0.0)	(0.0)	(0.0)	(0.0)	(0.0)	(0.0)
FB[b]	0.2	1.7		2.4	10.7		1.8	8.0	
	(0.1)	(2.6)	(8.1)	(2.2)	(10.1)	(24.2)	(1.6)	(7.8)	(18.8)

	Si			Ge		
	$n=1$	$n=2$	$n=3$	$n=1$	$n=2$	$n=3$
FC	0.0	0.0		0.0	0.0	
	(0.0)	(0.0)	(0.0)	(0.0)	(0.0)	(0.0)
RC	0.0	3.8		0.0	5.5	
	(0.0)	(2.6)	(9.1)	(0.0)	(2.8)	(10.6)
FB	2.4	12.7		1.9	10.7	
	(2.1)	(11.7)	(29.5)	(1.5)	(8.7)	(22.3)

[a] Data reported for B3LYP/CEP* geometries above, and B3LYP/MB geometries in parentheses below. [b] For $n = 1$, the relative energy of the boat conformer is reported, not the twist-boat; the latter is the zero of relative energy for the GaN system monomer.

We do note, however, that while we have emphasized the electrostatic contribution to curvature, there is certainly also a component in the heteroatomic rings associated with simple angle strain. A perfectly "flat" FC sheet is not compatible with significantly different bond angles subtended at X and Y atoms, and thus there is still more tendency for the GaN FC sheet to be rendered unstable. We now focus in more detail on the energetics associated with the various pseudo-2D motifs.

3.4. Energetic Trends of Pseudo-Two-Dimensional Expansion. Table 6 lists the relative energies of the FC, RC, and FB motifs at the B3LYP/CEP* and B3LYP/CEP*//B3LYP/MB levels of theory. For the monomers, where FC and RC both correspond to the chair conformer and FB is the boat conformer, the B3LYP/CEP* level is in good agreement with prior theoretical results for GaN,[14b] SiC,[26,36] GeC,[14b] and SiSi,[26,37] and also with experimental results for cyclohexasilane.[28] In general, the single-point energies computed for B3LYP/MB geometries are in good agreement with those computed for fully optimized geometries. The agreement is least good for GaN, consistent with the above analysis of dipole moments for these geometries. Nevertheless, the B3LYP/CEP*//B3LYP/MB energies for the GaN system with $n = 2$ are still fairly good despite the large deviation in geometries from B3LYP/CEP* compared to B3LYP/MB for this case (see Figure 4) suggesting that part of the reason for the large distortions with the smaller basis set is that the potential energy surface is not particularly sensitive to changes in the geometries of the outermost rings.

As the sheets increase in size, the FC motif becomes strongly favored in the SiSi and GeGe systems, consistent with the experimental observation of this motif in bulk systems.[34,35] This behavior is rationalized by the lack of torsional strain in these

systems coupled with the absence of any trans-diaxial interactions. The homoatomic nature of the rings guarantees that the interior valence bond angles will be well suited to expansion of the FC motif without introduction of angle strain. By $n = 3$, the preference for FC over RC is already quite large, and the FB structure, with its significant torsional strain and trans-diaxial interactions is strongly disfavored. The degree of separation in the motif energies is larger for SiSi than GeGe, consistent with the shorter bond lengths in the former compared to the latter.

In the SiC and GeC systems, by contrast, there is a reversal in the relative energies of the FC and RC motifs (the FB remains strongly disfavored). As noted above, part of this reversal is likely associated with electrostatics, since the dipole moments of the FC motifs are predicted to be significantly larger than the RC motifs. Two other components may be identified, however. First, the monomeric rings prefer a variation in interior ring bond angles at X and Y atoms of about 3 deg and a ring dihedral angle of about 53 deg. In the $n = 3$ FC structure, however, the nature of the sheet imposes a difference in bond angles of at most about 1 deg and a dihedral angle closer to 56 deg. This is in contrast to the corresponding geometric parameters in the $n = 3$ RC sheet, where greater variation in bond angles and smaller dihedral angles continue to be tolerated. That is, there is simply more flexibility in the RC motif.

Second, in the heteroatomic systems, the hydrogen atoms that come into closest contact in the RC and FB motifs are those attached to heavy atoms of different electronegativity. There is thus some opportunity for stabilization of these motifs by nontraditional H−H hydrogen bonding. This effect is probably rather small in the SiC and GeC cases, as judged by the FB energies relative to RC compared to the SiSi and GeGe systems (it is the FB systems that have the shortest H−H interactions between flagpole positions). However, it is evidently quite strong in the GaN case, given the very low relative energy of the FB motif (8.1 kcal mol^{-1}) for $n = 3$ compared to all other systems.[38]

This same nontraditional H−H hydrogen bonding appears to enhance the stability of the RC motif over the FC in the GaN case. In the RC geometry, each heavy atom that is axially substituted on another six-membered ring directs its attached hydrogen atom in such a way that it may form a bifurcated hydrogen bond with the hydrogen atoms having partial charges of opposite sign that substitute the other axial positions on the ring. The geometry of this interaction is sufficiently nonlinear that the term "hydrogen bond" may be too strong, but it is clear in any case that the electrostatic interaction is entirely favorable. In any case, the FC motif for GaN is predicted to be very strongly disfavored relative to the other possible forms.

3.5. Comparison of Pseudo-Two- and -One-Dimensional Systems for GaN and GeC. In earlier work we compared the electronic structures of pseudo-one-dimensional rods of isoelectronic GaN and GeC systems to one another (Figure 5).[8] These rods, which are formed by stacking six-membered ring chairs one atop another with extrusion of 3 equivalents of H_2 per connection and have the formula $H_3[(HXYH)_3]_nH_3$ (XY = GaN, GeC; $n = 1-9$), were furthermore characterized experimentally for the GaN case.[8] It is of interest to ask which structural form is preferred for a given XY system, a sheet or a rod, but a direct energetic comparison between them is not possible due to their different stoichiometries, nor does it prove possible to construct a simple isodesmic comparison,[12] since the two motifs do not incorporate new monomers in equivalent ways when they grow. However, we may take a simplified view of the energetics of these systems, similar in spirit to a molecular mechanics analysis. In particular, we hypothesize that the energies of the individual structures may be decomposed into contributions from two sets of substructures common to both, namely, HXYH fragments and pairs of H_2X/YH_2 fragments. We further assume that each of these substructural elements may be assigned a single intrinsic energy characteristic for a given motif. That is, the motif energy may be computed as

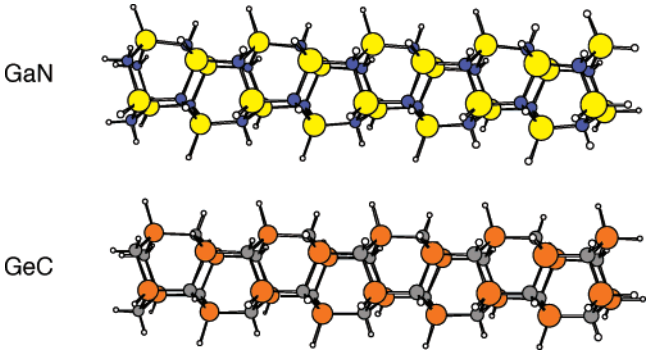

Figure 5. GaN and GeC rods of nine rings each optimized at the B3LYP/MB level.

TABLE 7: Relative Intrinsic Energies (kcal mol^{-1}) of HXYH and H_2X/YH_2 Segments (XY = GaN, SiC, GeC, SiSi, or GeGe) from Equation 1

		XY				
E_{rel}^{frag}	motif	GaN	SiC	GeC	SiSi	GeGe
HXYH	FC	0.0	0.0	0.0	0.0	0.0
	RC	−1.5	−0.4	−0.2	0.6	0.7
	FB	−1.1	0.6	0.6	1.3	1.0
	rod	−2.6		1.1		
H_2X/YH_2	FC	0.0	0.0	0.0	0.0	0.0
	RC	−1.2	0.2	0.1	−0.2	−0.3
	FB	−1.3	0.9	0.6	0.6	0.4
	rod	5.3		0.6		

$$E^{motif} = aE^{HXYH} + bE^{H_2X/YH_2} \quad (1)$$

In eq 1, E^{motif} is the electronic energy of a given FC, RC, or FB motif within the class of two-dimensional structures or, within the class of one-dimensional structures, of a given rod composed of from four to nine rings. In eq 1, coefficient a is the number of HXYH fragments in a particular structure. In the case of the two-dimensional motifs, we used the $n = 2$ and $n = 3$ structures for which cases $a = 6$ and 18, respectively (the monomer has no HXYH substructures and is not really representative of a particular type of structure); for the rods $a = 3n - 3$ where n is the number of monomers in the rod. Coefficient b is the number of pairs of H_2X and YH_2 fragments; its value is 6 and 9 for $n = 2$ and $n = 3$, respectively, in the 2D systems, and its value is 3 in all of the 1D systems.

The point of this analysis is that in a macroscopic system derived from effectively *infinite* expansion of the individual rod or 2D motif, both systems become composed exclusively of HXYH fragments. Hence, comparison of relative HXYH fragment energies permits comparison of rods to sheets in a balanced fashion. Table 7 contains the fitted fragment values expressed as relative energies. Note that in the case of the 2D sheets, since we use only the $n = 2$ and $n = 3$ energies, for any individual motif there are two equations in two unknowns and the fitted fragment energies are necessarily "exact". For the rods, however, there are six energies used in fitting the two coefficients. The root-mean-square errors of the energies predicted from the fit were 0.9 kcal mol^{-1} for the GaN rods and 0.2 kcal

mol^{-1} for the GeC rods. These relatively small errors serve to validate this simplified analysis.

The data in Table 7 indicate that the GaN rods are favored over any pseudo-two-dimensional motifs, while GeC rods are less favorable than *any* pseudo-2D motif. In the GaN case, this is consistent with the experimental observation that, under thermodynamic conditions, thermal ammonolysis of cyclotrigallazane results in rods and not sheets. As expected, this analysis also confirms that the favored sheet form for all other systems may be predicted from analysis of the relative HXYH fragment energies.

4. Conclusions

Hybrid density functional theory performs well in conjunction with effective core potentials in computing structures and energetics of group 13/15 and group 14/14 six-membered ring compounds. Larger sheet structures in which XY = GaN, SiC, or GeC compress and pucker the individual rings as concentric tori are added, while sheets with X = Y = Si and Ge expand and flatten the constituent rings. Energetically, the $[HGaNH]_n$ sheet prefers the combination of rolling cis- and trans-fused chairs over the flat boat conformation, with both being highly favored over the trans-fused flat chair motif. A significant portion of this preference is due to favorable interactions between hydrogens carrying partial charges of opposite sign (i.e., nontraditional H−H hydrogen bonds). Additional bias derives from angle and torsional strain imposed on the GaN system by the flat chair motif that is reduced in the other two options. $[HSiCH]_n$ and $[HGeCH]_n$ sheets also prefer the rolling chair motif, however the trans-fused chair is now preferred over the boat due in part to very much reduced favorable H−H interactions. The $[Si_2H_2]_n$, and $[Ge_2H_2]_n$ sheets prefer the trans-fused chair motif over the rolling chair, both of which are highly preferred over the boat, due to the lack of all torsional and trans-diaxial strain in these homoatomic ring systems.

Analysis of dipole moments indicates that electronic effects play a significant role in conformer preference for the GaN compounds, and that this effect is substantially diminished for the other less polar compounds studied here. Analysis of fragment contributions to the total energy of the pseudo-two-dimensional sheets and pseudo-one-dimensional rods suggests that poly(imidogallane) is thermodynamically more stable in the latter form, consistent with the experimental observation of this motif as a product from the thermal ammonolysis of cyclotrigallazane.

Acknowledgment. The National Science Foundation provided support for this work (Grant CHE02-03346). It is also a pleasure to acknowledge Professor Don Truhlar and to dedicate this paper to him as a part of this Festschrift. It has been a pleasure over the years to have been blessed with so stimulating and supportive a colleague, collaborator, and friend.

References and Notes

(1) Morkoc, H.; Mohammad, S. N. *Science* **1995**, *267*, 51.

(2) Ponce, F. A.; Bour, D. P. *Nature* **1997**, *386*, 351.

(3) (a) Han, W.; Fan, S.; Li, Q.; Hu, Y. *Science* **1997**, *277*, 1287. (b) Chen, X.; Li, J.; Cao, Y.; Lan, Y.; Li, H.; He, M.; Wang, C.; Zhang, Z.; Qiao, Z. *Adv. Mater.* **2000**, *12*, 1432. (c) Duan, X.; Lieber, C. M. *J. Am. Chem. Soc.* **2000**, *122*, 188. (d) Han, W.; Redlich, P.; Ernst, F.; Ruhle, M. *Appl. Phys. Lett.* **2000**, *76*, 652. (e) Li, J. Y.; Chen, X. L.; Qiao, Z. Y.; Cao, Y. G.; Lan, Y. C. *J. Cryst. Growth* **2000**, *213*, 408. (f) Tang, C. C.; Fan, S. S.; Dang, H. Y.; Li, P.; Liu, Y. M. *Appl. Phys. Lett.* **2000**, *77*, 1961. (g) Chen, C.-C.; Yeh, C.-C.; Chen, C.-H.; Yu, M.-Y.; Liu, H.-L.; Wu, J.-J.; Chen, K.-H.; Chen, L.-C.; Peng, J.-Y.; Chen, Y.-F. *J. Am. Chem. Soc.* **2001**, *123*, 2791. (h) Li, J.; Qiao, Z.; Chen, X.; Cao, Y.; He, M. *J. Phys.: Condens. Matter.* **2001**, *13*, L285. (i) Li, J. Y.; Chen, X. L.; Qiao, Z. Y.; Cao, Y. G.; Li, H. *J. Mater. Sci. Lett.* **2001**, *20*, 1987. (j) Shi, W. S.; Zheng, Y. F.; Wang, N.; Lee, C. S.; Lee, S. T. *Chem. Phys. Lett.* **2001**, *345*, 377. (k) Bae, S. Y.; Seo, H. W.; Park, J.; Yang, H.; Park, J. C.; Lee, S. Y. *Appl. Phys. Lett.* **2002**, *81*, 126. (l) Bae, S. Y.; Seo, H. W.; Park, J.; Yang, H.; Song, S. A. *Chem. Phys. Lett.* **2002**, *365*, 525. (m) Chang, K.-W.; Wu, J.-J. *J. Phys. Chem. B* **2002**, *106*, 7796. (n) Deepak, F. L.; Gundiah, G.; Govindaraj, A.; Rao, C. N. R. *Bull. Pol. Acad. Sci., Chem.* **2002**, *50*, 165. (o) Kim, H.-M.; Kim, D. S.; Park, Y. S.; Kim, D. Y.; Kang, T. W.; Chung, K. S. *Adv. Mater.* **2002**, *14*, 991. (p) Wang, J. C.; Feng, S. Q.; Yu, D. P. *Appl. Phys. A: Mater. Sci. Process.* **2002**, *75*, 691. (q) Choi, H.-J.; Johnson, J. C.; He, R.; Lee, S.-K.; Kim, F.; Pauzauskie, P.; Goldberger, J.; Saykally, R. J.; Yang, P. *J. Phys. Chem. B* **2003**, *107*, 8721. (r) Goldberger, J.; He, R.; Zhang, Y.; Lee, S.; Yan, H.; Choi, H.-J.; Yang, P. *Nature* **2003**, *422*, 599. (s) Hu, J.; Bando, Y.; Golberg, D.; Liu, Q. *Angew. Chem., Int. Ed.* **2003**, *42*, 3493. (t) Kuykendall, T.; Pauzauskie, P.; Lee, S.; Zhang, Y.; Goldberger, J.; Yang, P. *Nano Lett.* **2003**, *3*, 1063. (u) Lyu, S. C.; Cha, O. H.; Suh, E. K.; Ruh, H.; Lee, H. J.; Lee, C. J. *Chem. Phys. Lett.* **2003**, *367*, 136. (v) Xiang, X.; Cao, C.; Zhu, H. *Solid State Commun.* **2003**, *126*, 315.

(4) Jegier, J. A.; McKernan, S.; Gladfelter, W. L. *Inorg. Chem.* **1999**, *38*, 2726.

(5) Jegier, J. A.; McKernan, S.; Purdy, A. P.; Gladfelter, W. L. *Chem. Mater.* **2000**, *12*, 1003.

(6) Luo, B.; Gladfelter, W. L. *Inorg. Chem.* **2002**, *41*, 590.

(7) Luo, B.; Gladfelter, W. L. *Inorg. Chem.* **2002**, *41*, 6249.

(8) Kormos, B. L.; Jegier, J. A.; Ewbank, P.; Pernisz, U.; Young, V. G., Jr.; Cramer, C. J.; Gladfelter, W. L. *J. Am. Chem. Soc.* **2005**, *127*, 1493.

(9) Stephens, P. J.; Devlin, F. J.; Chabalowski, C. F.; Frisch, M. J. *J. Phys. Chem.* **1994**, *98*, 11623.

(10) Becke, A. D. *J. Chem. Phys.* **1993**, *98*, 5648.

(11) Becke, A. D. *Phys. Rev. A* **1988**, *38*, 3098.

(12) Cramer, C. J. *Essentials of Computational Chemistry*, 2nd ed.; John Wiley & Sons: Chichester, U.K., 2004.

(13) Lee, C.; Yang, W.; Parr, R. G. *Phys. Rev. B* **1988**, *37*, 785.

(14) (a) Cramer, C. J.; Gladfelter, W. L. *Inorg. Chem.* **1997**, *36*, 5358. (b) Campbell, J. P.; Hwang, J.-W.; Young, V. G., Jr.; Von Dreele, R. B.; Cramer, C. J.; Gladfelter, W. L. *J. Am. Chem. Soc.* **1998**, *120*, 521.

(15) (a) Timoshkin, A. Y.; Schaefer, H. F., III *Inorg. Chem.* **2004**, *43*, 3080. (b) Timoshkin, A. Y.; Schaefer, H. F., III *J. Am. Chem. Soc.* **2004**, *126*, 12141.

(16) Stevens, W.; Basch, H.; Krauss, J. *J. Chem. Phys.* **1984**, *81*, 6026.

(17) Stevens, W. J.; Krauss, M.; Basch, H.; Jasien, P. G. *Can. J. Chem.* **1992**, *70*, 612.

(18) Cundari, T. R.; Stevens, W. J. *J. Chem. Phys.* **1993**, *98*, 5555.

(19) Binkley, J. S.; Pople, J. A.; Hehre, W. J. *J. Am. Chem. Soc.* **1980**, *102*, 939.

(20) Hay, P. J.; Wadt, W. R. *J. Chem. Phys.* **1985**, *82*, 270.

(21) Wadt, W. R.; Hay, P. J. *J. Chem. Phys.* **1985**, *82*, 284.

(22) Hay, P. J.; Wadt, W. R. *J. Chem. Phys.* **1985**, *82*, 299.

(23) Hehre, W. J.; Stewart, R. F.; Pople, J. A. *J. Chem. Phys.* **1969**, *51*, 2657.

(24) Collins, J. B.; Schleyer, P. R.; Binkley, J. S.; Pople, J. A. *J. Chem. Phys.* **1976**, *64*, 5142.

(25) Frisch, M. J.; Trucks, G. W.; Schlegel, H. B.; Scuseria, G. E.; Robb, M. A.; Cheeseman, J. R.; Zakrzewski, V. G.; Montgomery, J. A., Jr.; Stratmann, R. E.; Burant, J. C.; Dapprich, S.; Millam, J. M.; Daniels, A. D.; Kudin, K. N.; Strain, M. C.; Farkas, O.; Tomasi, J.; Barone, V.; Cossi, M.; Cammi, R.; Mennucci, B.; Pomelli, C.; Adamo, C.; Clifford, S.; Ochterski, J.; Petersson, G. A.; Ayala, P. Y.; Cui, Q.; Morokuma, K.; Malick, D. K.; Rabuck, A. D.; Raghavachari, K.; Foresman, J. B.; Cioslowski, J.; Ortiz, J. V.; Stefanov, B. B.; Liu, G.; Liashenko, A.; Piskorz, P.; Komaromi, I.; Gomperts, R.; Martin, R. L.; Fox, D. J.; Keith, T.; Al-Laham, M. A.; Peng, C. Y.; Nanayakkara, A.; Gonzalez, C.; Challacombe, M.; Gill, P. M. W.; Johnson, B. G.; Chen, W.; Wong, M. W.; Andres, J. L.; Head-Gordon, M.; Replogle, E. S.; Pople, J. A. *Gaussian 98*, revision A.11.3; Gaussian, Inc.: Pittsburgh, PA, 1998.

(26) Arnason, I.; Oberhammer, H. *J. Mol. Struct.* **2001**, *598*, 245.

(27) Schmidbaur, H.; Rott, J.; Reber, G.; Mueller, G. *Z. Naturforsch. B* **1988**, *43*, 727.

(28) Smith, Z.; Almenningen, A.; Hengge, E.; Kovar, D. *J. Am. Chem. Soc.* **1982**, *104*, 4362.

(29) Huheey, J. E.; Keiter, E. A.; Keiter, R. L. *Inorganic Chemistry: Principles of Structure and Reactivity*, 4th ed.; Harper Collins: New York, 1993. See also http://www.webelements.com.

(30) Bent, H. A. *Chem. Rev.* **1961**, *61*, 275.

(31) Pauling, L. *The Nature of the Chemical Bond*; Cornell University Press: Ithaca, NY, 1960.

(32) Crabtree, R. H.; Siegbahn, P. E. M.; Eisenstein, O.; Rheingold, A. L.; Koetzle, T. F. *Acc. Chem. Res.* **1996**, *29*, 348.

(33) Custelcean, R.; Jackson, J. E. *Chem. Rev.* **2001**, *101*, 1963.

(34) (a) Dahn, J. R.; Way, B. M.; Fuller, E. *Phys. Rev. B* **1993**, *48*, 17872. (b) Dettlaff-Weglikowska, U.; Hönle, W.; Molassioti-Dohms, A.; Finkenbeiner, S.; Weber, J. *Phys. Rev. B* **1997**, *56*, 13132.

(35) Vogg, G.; Brandt, M. S.; Stutzmann, M. *Adv. Mater.* **2000**, *12*, 1278.

(36) Arnason, I.; Thorarinsson, G. K.; Matern, E. *J. Mol. Struct. (THEOCHEM)* **1998**, *454*, 91.

(37) Leong, M. K.; Mastryukov, V. S.; Boggs, J. E. *J. Phys. Chem.* **1994**, *98*, 6961.

(38) In organic−inorganic hybrid single crystals that do *not* include hydrogen atom caps at each position (and thus do not suffer from flagpole interactions) the FB motif has been observed in several instances for the inorganic component, e.g., CdChalcogen: (a) Deng, Z.-X.; Li, L.; Li, Y. *Inorg. Chem.* **2003**, *42*, 2331. (b) Huang, X.; Li, J.; Zhang, Y.; Mascarenhas, A. *J. Am. Chem. Soc.* **2003**, *125*, 7049. ZnS: (c) Ouyang, X.; Tsai, T.-Y.; Chen, D.-H.; Huang, Q.-J.; Cheng, W.-H.; Clearfield, A. *Chem. Commun.* **2003**, 886. ZnSe: (d) Fu, H.; Li, J. *J. Chem. Phys.* **2004**, *120*, 6721. ZnTe: (e) Li, Y.; Ding, Y.; Wang, Z. *Adv. Mater.* **1999**, *11*, 847. (f) Huang, X.; Li, J.; Fu, H. *J. Am. Chem. Soc.* **2000**, *122*, 8789. ZnSe and MnSe: (g) Huang, X.; Heulings, H. R., IV.; Le, V.; Li, J. *Chem. Mater.* **2001**, *13*, 3754.